Protective Effects of Swertiamarin against Methylglyoxal induced Damage and its Role in Preventing Diabetic Nephropathy by Improving Oxidative Stress in Rat Kidney Epithelial (NRK-52E) Cells

Kirti Parwani
Department of Biological Sciences, P D Patel Institute of Applied Sciences, Charotar University of Science and Technology, Changa, Anand, Gujarat

Farhin Patel
Department of Biological Sciences, P D Patel Institute of Applied Sciences, Charotar University of Science and Technology, Changa, Anand, Gujarat

Dhara Patel
Department of Biological Sciences, P D Patel Institute of Applied Sciences, Charotar University of Science and Technology, Changa, Anand, Gujarat

Palash Mandal (palashmandal.bio@charusat.ac.in)
Department of Biological Sciences, P D Patel Institute of Applied Sciences, Charotar University of Science and Technology, Changa, Anand, Gujarat

Research Article

Keywords: Enicostemma littorale, Swertiamarin, Advanced glycation end product (AGE), AGE-inhibitor, Diabetic Nephropathy

Posted Date: December 14th, 2020

DOI: https://doi.org/10.21203/rs.3.rs-123927/v1

Abstract

Increased blood glucose in diabetic individuals results in the formation of advanced glycation end products (AGEs), which result in various adverse effects on kidney cells, leading to diabetic nephropathy (DN). In this study, the antiglycative potential of Swertiamarin (SM) isolated from the methanolic extract of *E. littorale* was explored. The effect of SM on protein glycation was studied by incubating bovine serum albumin with fructose at 60 °C in the presence and absence of different concentrations of swertiamarin for 24 h. For comparative analysis, metformin was also used at similar concentrations as SM. Further, to understand the role of SM in preventing DN, in vitro studies using NRK-52E cells were done by treating cells with methylglyoxal (MG) in the presence and absence of SM. SM showed better antiglycative potential as compared to metformin. Also, SM could prevent the MG mediated pathogenesis in DN by reducing levels of argpyrimidine, oxidative stress and apoptosis in kidney cells. SM also downregulated the expression of interleukin-6, tumor necrosis factor-α and interleukin-1β. This study, for the first time, reports the antiglycative potential of SM and also provides a novel insight into the molecular mechanisms by which SM prevents toxicity of MG on rat kidney cells.

Introduction

Type 2 Diabetes (T2D) is a metabolic syndrome, which results due to peripheral insulin resistance, affecting both, metabolism and disposal of glucose. The occurrence of diabetes is accelerating worldwide, with a consequent increase in secondary complications like diabetic nephropathy (DN), neuropathy, retinopathy, and cardiovascular complications. Hyperglycaemia is one of the main reasons for causing DN, and various clinical trials have established that the progression to DN can be slowed and also reversed by good and strict glycemic controls [1–3]. Elevated blood glucose, which induces reactive oxygen species (ROS) formation, is understood to be one of the main reasons for the AGEs formation in the intracellular and extracellular environment [4]. AGEs are the products of non-enzymatic glycation between free amino acids and reducing sugar via the Maillard reaction resulting into yellowish-brown fluorescent and insoluble adducts. The formation of AGEs is divided into two stages. In the earlier stage, Amadori product, a stable compound is formed from an unstable Schiff base [5]. Amadori products can either form reactive diacrbonyls like glyoxal and methylglyoxal (MG) or upon several other chemical reactions like condensation, dehydration, oxidation, etc., can undergo formation of AGEs. These adducts can alter the normal physiological functions of a protein upon glycation [6]. This can alter the half-life of the proteins and affect their physiological clearance. Of late, patients with persistent T2D are established to have vastly higher levels of AGEs [7]. The role of AGEs in DN has been documented by reports suggesting the negative correlation between the accumulation of AGEs in plasma and renal function [8]. AGEs bind to their receptor called receptor for advanced glycation end products (RAGE) and primarily leads to the generation of ROS and oxidative stress which further leads to the damage of the renal tubular cells and mesangial cells leading to DN. Further, AGEs lead to an imbalance between synthesis and degradation of extracellular matrix components like collagen and cause their accumulation in the

mesangium, tubular interstitial cells, and glomerulus basement membrane leading to their hardening, which is a hallmark feature of DN [9].

Reduced antioxidant defenses have also been reported in diabetic patients thereby providing acceleration to the development of chronic complications [10]. It is reported that AGEs could alter the physiological functions of an anti-oxidant enzyme like superoxide dismutase (SOD) and could inactivate it [11]. Glycation has been found to induce aggregation and structural modifications in catalase by targeting lysine residues [12]. This reduced antioxidant machinery along with increased ROS due to hyperglycaemia can be detrimental for a cell. Many synthetic inhibitors that can restrain the formation of AGEs have been identified and studied but they have been withdrawn back due to their lower potency and side effects. Therefore, there arises a rationale to identify some inhibitor, which along with being potent and effective, should have low toxicity.

Traditional and herbal therapies are gaining importance slowly over conventional medicines due to their advantage of having lower or no side-effects. The molecules present in the plants are shown to be hypoglycaemic, hypolipidemic, and anti-oxidant in nature. Compounds in the plants like phenolics [13], polysaccharides [14] carotenoids [15], etc. are shown to possess anti-glycating properties. Also, the regular consumption of edible products rich in anti-oxidants and polyphenolic compounds could be beneficial in the prevention of diabetes and related complications [16]. *Enicostemma littorale* commonly called Mamejava has been shown to possess a hypoglycaemic effect in T2D rats [17]. *E. littorale* contains important phytoconstituents like gentianine, enicoflavine, gentiocrucine, swertiamarin, etc. to name a few. Swertiamarin (SM) has been shown to possess anti-cholinergic [18], anti-hyperlipidaemic [19] hypoglycaemic [20] and antioxidant effects [21].

Since glycation is a process associated with increased free radical formation, compounds with antioxidant activities could also act as an inhibitor of the formation of AGEs [22]. Given the important role of SM in diabetes mellitus and its antioxidant potential, the present study was executed to understand and assess its antiglycation potential. To our knowledge, this is the first report that shows inhibition of fructose mediated glycation by SM and also its protective role in MG induced damage on kidney cells, thereby preventing DN.

Materials And Methods

Isolation of SM

The dry plant *E.littorale* was acquired from Saurashtra region, Gujarat, India . The plant was press dried and then powdered in a crusher. The powder was immersed overnight in double the volume of 70% methanol (SRL, India) and 30% water. The process was repeated for three times for a single batch and then filtered. The filtrate was vacuum evaporated using a rotary evaporator (Heidolph Germany), to get a dry hydro-alcoholic extract.

To obtain SM from the hydro-alcoholic extract, silica based column chromatography was done. 1 g of hydro-alcoholic extract was coated with 3 g silica. The extract was chromatographed using silica gel (60 -120 mesh size, Merck , Germany) with hexane and then with hexane containing ethyl acetate (60-97 %), followed by ethyl acetate and then with ethyl acetate mixed with methanol in the order of increasing polarity (0.5-1.5%). Fractions with different polarities were assessed for the presence of SM by thin-layer chromatography (TLC) using the solvent system of chloroform: methanol (8:2). The presence of SM was established by co-chromatography of the standard SM (TCI, Japan) along with different fractions. Fractions with SM were pooled and dried. They were further purified by precipitating the methanol dissolved residue with non-polar solvents like diethyl ether (yield: 7%).

Characterization of the Isolated SM

The characterization as well as the purity of the isolated compound was confirmed by various methods which included TLC , HPLC, LC-MS and FTIR.

High Performance Liquid Chromatography (HPLC)

For HPLC analysis, the solution of SM isolated in the lab was prepared to achieve a final concentration of 1 mg/ml in methanol. The samples and solvents to be used as mobile phases were filtered through 0.2 µm syringe filters (Axiva, India). HPLC was carried out using the previously described mobile phase for SM with slight modifications by using acetonitrile: water (10:90) as the mobile phase [23]. The flow rate was 1 ml/min and the column temperature was maintained at 25°C. The detection wavelength and mode for SM was 238 nm and Photodiode detector (PDA).

Fourier-transform infrared spectroscopy (FTIR) and mass spectrometer (MS)

The isolated compound was analyzed by FTIR for the identification of functional groups present in the compound. The standard was also used as a reference for the isolated compound. A homogenous solution of both, standard and the compound was individually prepared in potassium bromide (KBr) and subjected to FTIR spectrophotometer (Thermofisher Scientific, USA). The compound isolated was also subjected to positive- ion Electrospray Ionization i.e. ESI using Perkin – Elmer Applied Biosystem Sciex API 2000 for identification of its characteristic molecular ion peak.

In-vitro Antiglycative Studies

Antiglycative studies were done as suggested by McPherson et al. with slight modifications [24]. Bovine Serum Albumin (BSA, Himedia, India) and Fructose (Merck, USA) were used to induce glycation. In brief,

in a 1.5 ml eppendorf, 100 µl of 60 mg/ml BSA (20 mg/ml final concentration) was incubated with 100 µl of 1.5 M fructose (0.5 M final concentration) and 100 µl of potassium phosphate buffer (pH 7.4). Negative control was incorporated as well, which consisted of 100 µl of 60 mg/ml BSA (20mg/ml final concentration) and 200 µl of potassium phosphate buffer (pH 7.4). To understand the antiglycative potential of the compound, the same reaction was carried out in the presence of varying concentrations of SM (1 µg/ml to 10 µg/ml). For the comparative studies, metformin was used as a positive antiglycative control at the same concentrations as of SM. The reaction was incubated at 60°C for 24 h and samples were analyzed for fluorescence due to AGEs on a spectrofluorometer (Perkin Elmer LS-55, USA) by using an excitation wavelength of 370 nm and an emission wavelength of 440 nm.

UV Absorbance Spectroscopy

The native, glycated BSA and samples in which BSA glycated in presence of SM were analyzed for their absorption spectra on Shimadzu UV-1700 spectrophotometer in 200 to 800 nm wavelength range using a quartz cuvette. The samples were analyzed for the hyperchromic shift due to glycation by fructose as suggested by Allarakha et al [25].

Culturing of NRK-52 E Cells

Normal Rat Kidney (NRK-52E) cell line was acquired from National Centre for Cell Sciences (NCCS), Pune, India. The cells were cultured in Dulbecco's Modified Eagle Medium Low Glucose (5.5 mM/L) medium with 10% fetal bovine serum, 1% L-glutamine, and 1% penicillin/streptomycin (Thermofisher Scientific, USA) at 37 °C in a 5% CO_2 incubator. The cells were grown till 80-90% confluency, after which they were used for experiments with high glucose in the presence and absence of SM.

Cell Viability Assay

The concentration of methylgloxal (MG) (Sigma-Aldrich, USA) used during the experiments was determined by checking MG toxicity on NRK-52E cells using 3-(4,5-dimethylthiazol-2-yl)-2,5-diphenyltetrazolium bromide (MTT) assay described by Riss et al [26]. In brief, $1X10^4$ cells were seeded in a 96-well plate. After 24 h, cells were exposed to different concentrations MG (1 mM, 500 µM, 250 µM, 125 µM, 62.5 µM, 31.25 µM, 15.625 µM, 7.812 µM, and 3.906 µM), along with an untreated control well, for 24 h . After treating them for 24 h, 10 µl of MTT solution was added to each well at a final concentration of 0.5 µg/ml, and cells were incubated at 37°C in a 5% CO2 atmosphere for 3 h in the dark. Following the incubation period, formazan crystals formed in each well were solubilized using 100 µl dimethyl sulfoxide (DMSO) solution. The absorbance was then measured at 570 nm to determine the viability of cells.

MG Stimulation and Different Treatment Groups

To check the effect of MG on NRK-52E cells, 8 X 10^5 cells were seeded in a 60 mm culture plates followed by incubation for 24 h. After this, cells received different treatments based on the respective groups like control (only growth medium), MG (medium containing 200 µM MG), and MG + SM 100 µg/ml (medium containing 200 µM MG in the presence of 100 µg/ml SM). The effect of MG-induced stress on kidney cells was assayed by checking the ROS production, lipid peroxidation, argpyrimidine levels, DNA damage, and transcript levels of various genes involved in the progression of DN by qRT PCR.

Estimation of Argypyrimidine

To estimate the levels of argypyrimidine, NRK-52E cells (8×10^6 cells/well) were seeded onto 60mm plates, and the cells were incubated for 24 h. After 24 h, cells were treated with MG, in the presence and absence of SM for 24 h. After the incubation, the cells were lysed using the lysis buffer followed by centrifugation at 16000 rpm for 10 min at 4°C. The supernatant was then analyzed using a fluorescence spectrophotometer (Hitachi, F-7000) with an excitation wavelength of 330 nm and an emission wavelength of 380 nm for the presence of argypyrimidine [27].

ROS Estimation

In order to estimate oxidative stress caused by MG in the presence or absence of SM, the cells were treated with 200 µM MG alone or along with SM and incubated for 24 h. After treatment, cells were incubated with 5(6)-carboxy-20,70-dichlorofluorescein Diacetate (Carboxy-H2-DCFDA) (Sigma-Aldrich, USA) in the dark with a final concentration of 30 µM at 37^0C for 1 h. The cells were then harvested, washed with PBS, and resuspended in PBS. ROS production in the cells was measured by measuring the fluorescence of the sample at an excitation wavelength - 485 nm and an emission wavelength - 530 nm, using a fluorescence spectrophotometer (Perkin Elmer LS-55, USA [28].

MDA estimation in cells by HPLC

Total malondialdehyde (MDA) in the cultured cells was estimated using HPLC by following the method described by Tukozkan et al with some modifications [29]. Summarily, the medium was removed from the plates and the cells were rinsed with PBS. Cells were homogenized in cold 1.15% KCl to make 10% homogenate. 500 µl of the homogenate was then mixed with 100 µl of 6 M NaOH, and the samples were incubated in a water bath at 60°C for 45 min. The hydrolyzed sample was then acidified with 250 µl of 35% perchloric acid. The samples were subjected to centrifugation at 15000 g for 10 min. After centrifugation, 250 µl of the supernatant was collected and mixed with 25 µl of DNPH solution, followed by 10 min incubation in the dark. The samples were then analyzed by HPLC in an ODS2 reverse column using acetontitrile: water (38:62) containing 0.2% acetic acid as a mobile phase. Isocratic conditions were

maintained during HPLC with a flow rate of 1 ml/min and the MDA was detected in the samples at 310 nm with the UV detector with a retention time of about 10 min. The concentration of MDA was detected in the sample by comparing it with the standard curve prepared using 1,1,3,3 tetraethoxypropane.

DNA damage by Comet Assay

To see if MG can induce DNA damage, cells received respective treatments as mentioned earlier for 24 h followed by comet assay as described previously by Fazeli et al with little modifications [30]. In brief, the cells after having mixed with low melting agarose were loaded on a frosted microscopic slide having a thin layer coat of high- melting point agarose. Cells were lysed by immersing the slides in lysing solution containing Triton X-100 (1%), DMSO (10%), and 89% lysis buffer (composition: 10mM Tris, pH 10; 1% Na-sarcosine; 2.5M NaCl and 100mM Na_2EDTA) followed by incubation at 4°C in the dark for 1 h. The unwinding of DNA was permitted in alkaline electrophoresis buffer (composition: 300mM NaOH and 1mM Na_2EDTA, pH 13) for 20 min at 4°C in the dark, followed by electrophoresis at 4°C, for 20 min under 1 V/cm and 300 mA electrical field. After the electrophoresis, the slides were neutralized in a neutralization buffer (0.4 M Tris, pH 7.5) for 5 minutes. The slides were then stained with 1 X Ethidium Bromide (10X stock of 20 µg/ml) for 5 min, followed by washing with chilled distilled water to remove excess stain. The DNA damage was observed under the fluorescence microscope and the DNA damage was analyzed using the percentage tailing of the DNA.

qRT-PCR

After the respective treatments and incubation period, total RNA was isolated from the cells using Trizol reagent (Invitrogen, USA) as per the manufacturer's instructions. RNA was quantified using nanodrop (Thermofisher Scientific, USA) and 1 µg of total RNA was used to synthesize cDNA using a high capacity cDNA synthesis kit (Applied Biosystems, USA) as per the manufacturer's protocol. The mRNA expression of various genes under the investigation was done using PowerUp SyBr green master mix (Applied Biosystems, USA) in an Agilent Mx3005P qRT-PCR system. The cycle conditions for the qRT-PCR are (a) initial denaturation for 10 min at 95°C followed by (b) 40 repeats of denaturation at 95°C for 30 s, (c) annealing time of 1 min at 60°C and (d) extension at 72 °C for 1 min. The fold change in the expression of the genes was calculated using the $2^{-\Delta\Delta Ct}$ method using 18s rRNA as an endogenous control. The list and the sequence of the primers used are shown in Table 1.

Table 1
Primer sequences of the genes under investigation

Gene	Forward Primer Sequence	Reverse Primer Sequence
18 S	5'ACGGAAGGGCACCACCAGGA 3'	5'CACCACCACCCACGGAATCG 3'
RAGE	5' GGTACTGGTTCTTGCTCT 3'	5'ATTCTAGCTTCTGGGTTG 3'
TNF-α	5' CAAGGAGGAGAAGTTCCCAA 3'	5'CTCTGCTTGGTGGTTTGCTA 3'
ICAM-1	5'CCCCACCTACATACATTCCTAC 3'	5'ACATTTTCTCCCAGGCATTC 3'
NADPH Oxidase	5' GGCATCCCTTTACTCTGACCT 3'	5' TGCTGCTCGAATATGAATGG 3'
IL-6	5' GCCCTTCAGGAACAGCTATGA 3'	5'TGTCAACAACATCAGTCCCAAGA 3'
CYP2E1	5' CTTCGGGCCAGTGTTCAC 3'	5' CCCATATCTCAGAGTTGTGC 3'
TGF-β	5' – TGCTTCAGCTCCACAGAGAA 3'	5' TGTGTTGGTTGTAGAGGGCA 3'
IL-1β	5' CCCTGCAGCTGGAGAGTGTGG 3'	5' TGTGCTCTGCTTGAGAGGTGCT 3'

Statistical analysis

All experiments were repeated at least thrice. Data were presented as mean ± SEM of three different experiments, analyzed using GraphPad Prism 6 software (GraphPad Software Inc., La Jolla, CA). Differences between groups were analyzed using one-way analysis of variance with Tukey's multiple comparisons test. A *p* value less than 0.05 was considered significant.

Results

The isolated compound was characterized and identified as SM when compared to standard SM.

SM was successfully isolated from *E. littorale* as confirmed by TLC. By our isolation method, we report 7% yield of SM from the methanolic extract of *E. littorale*, which to our knowledge is the highest yield obtained till now.

The presence of SM was confirmed with reference to the standard SM using the chloroform: methanol (8:2 v/v) as a mobile phase with R_f of 0.58. The visualization was done at 254 nm as shown in Figure 1a.

High-Performance Liquid Chromatography (HPLC) analysis of SM

The HPLC profiles of the isolated SM (a) and the standard (b) are shown in Figure 1b . Both the standard and the lab isolated SM gave a characteristic peak at 238 nm, which is the absorbance maxima of SM as reported earlier. The retention time of the lab isolated SM was found to be 3.801 which fairly matched to 3.805 of that of the standard with the acetonitrile: water (10:90) as the mobile phase.

Identification of functional groups of SM through fourier-transform infrared spectroscopy (FTIR)

The lab isolated SM fairly matched the FTIR spectrum of the standard SM (Fig. 1c). FTIR spectra of both, isolated and standard swertiamrin showed definite peaks between wavenumbers 4000–500 cm^{-1}. The characteristic O-H stretch peak was found at 3381 cm^{-1}, C-H stretch at 2292 cm^{-1}, C=O stretch at 1694 cm^{1}, C=C stretch at 1617 cm^{-1} C-O-C at 1411 $cm^{-1,}$ and C=CH_2 stretch at 844 $cm^{-1.}$ This validates the purity of the isolated compound as the wavenumbers for both compounds (lab isolated and standard SM) match with each other.

Liquid chromatography-mass spectra(LC-MS) fingerprint of SM

The LC-MS spectrum of SM reported earlier showed a molecular ion peak at m/z of 374, but LC-MS spectrum for SM isolated in our lab as shown in Figure 1d, showed m/z of 375.1 in positive ion mode, indicating the addition of H^+ to the compound, thereby increasing molecular ion peak by 1, as shown in Merck Index.

SM inhibited the formation of AGEs

AGEs being molecules with a characteristic property of fluorescence after glycation were measured at excitation and emission wavelengths of 370 nm and 440 nm respectively. The fluorescence intensity was used as a measure of glycation i.e. higher the intensity of fluorescence, the higher is the glycation of proteins. The intensity of fluorescence was significantly decreased ($p \leq 0.0001$)in SM treated samples as compared to untreated samples that contained neither SM nor metformin. Also, SM could inhibit the formation of AGEs better than metformin ($p<0.0001$)at similar doses (Figure 2). This indicates that SM could be better in preventing the formation of endogenous AGEs due to persistent hyperglycaemia in diabetic subjects.

SM reduces fructose mediated hyperchromicity

The changes in the structure of BSA and its absorbance were additionally analyzed by spectrophotometer (Fig. 3a). As shown in Figure 3b, compared to normal BSA (Black line), glycated BSA (Blue line) shown increased absorbance and hyperchromicity (89 %) due to fructose mediated changes in the structure of BSA. SM could prevent the fructose mediated changes in the BSA (Green line) as depicted by reduced hyperchromicity (57.9 %) indicating the inhibition of glycation (p<0.0054) (Fig.3c).

Effect of MG on NRK-52E cell viability

The toxicity of MG on NRK-52E cells was analyzed for fixing the dose for further experiments on NRK-52E. The dose-dependent decrease in cell viability is observed with an increase in the MG concentration (p <0.0001) (Fig. 4a). Approximately more than 60 % of cell viability was observed at 250 µM MG concentration, therefore, 200 µM was considered as the final concentration for further experiments with MG on NRK-52E cells. The effect of MG on the morphology of NRK-52E cells can be seen in Figure 4b. MG treatment on the cells changed the cobblestone morphology of NRK-52E cells to a round and elongated fibroblast-like shape, indicating the cellular damage due to MG, which was prevented when cells were treated with MG along with SM.

SM alleviates the formation of argpyrimidine

Dicarbonyls like MG react with arginine in the proteins to form AGEs and argpyrimidine is a major modification of amino acid arginine by MG. As shown in Fig.5, NRK-52E cells when treated with MG shown higher levels of argpyrimidine as compared to the untreated cells. The treatment of SM along with MG alleviated the levels of argpyrimidine which could be due to the inhibition of modification of arginine by MG, thereby reducing the glycation induced damage to the cells.

Effect of SM on ROS production

The production of ROS was analyzed in the NRK-52E cells treated with MG alone or in presence of SM using a fluorescence spectrophotometer as shown in Figure 6b. The treatment with MG induced the formation of ROS which was prevented by SM treatment with MG (p<0.01) , suggesting the quenching of MG-induced free radicals by SM.

SM mitigates MG induced oxidative stress

Oxidative stress was assessed by the formation of MDA, a molecule that is formed due to lipid peroxidation of the cells, caused by the generation of excessive free radicals. MDA was found to be higher in the cells treated with MG after 24 h (as seen by MDA peak in Figure 6a). The treatment with 100

µg/ml SM along with MG for the same duration, could show lower levels of MDA as compared to the cells treated with MG alone. This shows that 24 h treatment can effectively reduce the formation of MDA, which manifests in the cells due to MG and hyperglycaemia.

Effect of SM in MG induced cell death in NRK-52E cells

MG exposure to NRK-52E cells led to morphological changes in the cells, which reflected the cells undergoing apoptosis. Upon checking for the apoptosis by comet assay, cells treated with MG for 24 h, showed higher DNA damage as concluded by % tailing of DNA. Co-treatment of cells with MG and 100 µg/ml SM showed a relatively lower degree of DNA damage after 24 h of incubation (p<0.0001)(Figure 7a and 7b). This shows that SM can prevent the DNA damage induced due to MG toxicity and hence can prevent NRK-52E cell death.

SM ameliorates MG induced inflammation and epithelial-mesenchymal transformation (EMT) in NRK-52E cells

Cells when treated with MG caused elevated levels of oxidative stress which resulted in the upregulation of ROS, thereby inducing the expression of CYP2E1 in NRK-52E cells. However, CYP2E1 mRNA expression was comparatively reduced when the cells were treated with 100 µg/ml SM along with MG exposure. mRNA expression of inflammatory marker like NADPH oxidase, and various pro-inflammatory cytokines like interleukin-6 (IL-6), tumor necrosis factor-α (TNF- α), and interleukin-1β (IL-1 β) was upregulated in cells treated with MG. Nonetheless, SM treatment at a concentration of 100 µg/ml to MG exposed cells could prevent the upregulation of all the inflammatory cytokines under investigation (p<0.0001; p<0.001; p<0.01), therefore explaining the preventive role of SM in inflammation of kidney cells.

MG, being one of the intermediates to the formation AGEs, can also upregulate the receptor for advanced glycation end products (RAGE), a membrane-bound receptor found on kidney cells. We found the higher mRNA expression levels of RAGE in MG treated cells, which was ameliorated when the cells were treated with both SM along with MG as compared to the cells treated with MG alone. The expression of cellular endothelial factor-like intracellular adhesion molecule – 1 (ICAM-1) was also found to be reduced in the cells treated with SM along with MG as compared to the cells exposed to MG alone (p<0.05) .

NRK-52E cells when treated with MG, showed morphological changes and the epithelial nature of cells changed to elongated, and fibroblast-like phenotype (Figure 4b), maybe due to epithelial-mesenchymal transformation (EMT). SM treated group, did not show any change in the epithelial morphology of NRK-52E cells. It is previously reported that transforming growth factor- β (TGF- β) plays a very crucial role in the pathogenesis of DN, which in our study, showed upregulated expression in the cells treated with MG as compared to cells co-treated with MG and SM. However treatment of SM along with MG could

alleviate TGF- β expression in NRK-52E cells (p<0.001). Figure 8 shows the mRNA expression profile of all the genes under investigation.

Discussion

In the present study, we report isolation of SM and its role in inhibiting the formation of AGEs. The SM was isolated in the lab from *E. littorale* with better yield (7%) by column chromatography, which to our knowledge is the highest yield using silica of 60–120 mesh size. The absorbance maxima in the HPLC of isolated SM matched with the absorbance maxima of the SM isolated by Rana et al and with the UV spectral analysis by Vishwakarma et al to be at 238 nm [31, 32]. The molecular ion peak of the isolated SM was 375.1 which matched with the results obtained in literature along with their FT-IR fingerprint, proving the compound to be SM [33]. Owing to various properties like anti-cholinergic [18] anti-hyperlipidaemic [19] and given the important role of SM in diabetes mellitus [20] and its antioxidant potential [34], the present study was executed to understand and assess its antiglycation potential.

The persistent hyperglycaemia in the blood leads to the production of ROS which results in oxidative stress. Oxidative stress results not only due to excessive ROS but may also result due to defects or impairment in the antioxidant enzymes which otherwise can clear the ROS[35]. Increased blood glucose exacerbates the formation of ROS and is one of the prime reasons for AGEs formation, which further leads to various complications of T2D like DN [36–38]. Free radicals can induce the formation of AGEs from Amadori products [39]. This is explained by the study which shows the increased levels of MG in the blood of diabetics as compared to non-diabetic individuals [40] and also supported by a study proving the accumulation of AGEs in most DN patients [41]. Under diabetic conditions, the excess of glucose leads to the activation of polyol pathway, resulting in the formation of fructose [42]. Fructose leads to the formation of AGEs and ROS by promoting the glycation of proteins and lipids, also aided by MG which is a dicarbonyl fomed during glycolytic pathway for glucose metabolism [43]. Hence, preventing the glycation induced by fructose and MG could be one of the prime strategies to inhibit the formation of AGEs and prevent the diabetes related complications [44].

We, therefore assessed the potential of SM in inhibiting the fructose induced glycation. Fructose mediated glycation of proteins increases their fluorescence intensity at 440 nm which is due to formation of AGEs [45]. In the present study, BSA glycated with fructose showed increased fluorescence intensity as compared to BSA treated with fructose in presence of SM, which explains the role of SM in being able to prevent the formation of AGEs. To understand the potency of SM in being able prevent the formation of AGEs, we compared it with metformin which is already known to prevent MG mediated glycation of albumin and also prevent renal tubular injury [46, 47].SM at similar dose to that of metformin could significantly inhibit the formation of AGEs much better as compared to metformin, which proves it to a better glycation inhibitor than metformin. The glycation induced by fructose leads to modifications of various proteins, which renders the loss of function of proteins. This can be understood by hyperchromicity that can be attributed to the loss or fragmentation of the proteins, which causes the exposure of the aromatic amino acids responsible for its higher absorption at 280 nm [48]. It is of prime

importance to understand the changes in the proteins caused due to their frutosylation, as the concentration of fructose increases up to as high as 5 mM in the kidneys and peripheral nerves due to polyol pathway [49]. Our results show that the fructose mediated glycation was prevented when the glycation of BSA by fructose was carried out in presence of SM, as seen by reduced hyperchromicity which indicates the role of SM in preventing the fructose or AGEs mediated damage to kidney cells.

As discussed earlier, AGEs lead to the formation of ROS, which results in the oxidative stress. The formation of ROS and the repair of the damage caused due to ROS and oxidative stress is normally rescued in the cells by its antioxidant enzyme machinery comprising of antioxidant enzymes like catalase and SOD. However, glycation of enzymes like catalase and SOD lead to the loss of their activity, rendering an imbalance in homeostasis of oxidants and anti-oxidants in the cell [50]. ROS being toxic to kidney cells promote cell death by inflammatory and fibrogenic reactions in the kidney cells [51]. Therefore, to understand the cellular effects of AGEs and how SM could prevent AGEs mediated progression of DN, we used an *in-vitro* MG-induced model of DN. The concentration of MG to be used in the study was determined using MTT based cell viability assay. The dose-dependent decrease in the cell viability was observed as MG with increasing concentration may have induced apoptosis in the cells. Since nearly 40% cell death was observed at 250 μM concentration of MG, we chose 200 μM MG concentration for our further experiments, which was supported by studies on rat mesangial cells, where 200 μM MG resulted in apoptosis of mesangial cells after 8 h of incubation with MG [52]. MG in particular can act as a source to the formation of a specific fluorescent AGE called Argpyrimidine, which is formed by a reaction of MG with the guanidine group of arginine [27]. Argpyrimidine was also found to be accumulated in the intima and media of small arteries of the kidneys of diabetic patients, which suggested its role in the progression of DN[53]. Approximately two to three-fold higher levels of argpyrimidine are found in diabetic patients as compared to non-diabetic individuals. The argpyrimidine levels also are found to positively correlate with glycosylated haemoglobin [27]. Higher levels of argpyrimidine were found to be present in the mesangial cells of rat kidney cultured in high glucose-containing medium [54]. Our study shows that SM can prevent the formation of AGEs and in specific could also inhibit the formation of MG mediated argpyrimidine formation in NRK-52 E cells. We also found increased levels of ROS in MG treated cells which as discussed earlier could be possibly due to the formation of AGEs [39]. However the cells treated with SM along with MG showed reduced ROS, suggesting the anti-glycative property of SM.

It is well established that oxidative stress and increased free radical can induce lipid peroxidation. This is because lipids are most vulnerable to the attack by ROS and reactive nitrogen species [55]. This can generate increased levels of MDA, which is one of the major mutagenic and toxic products formed during the process of lipid peroxidation [56]. The present study shows that co-treatment of NRK-52E cells with MG and SM, reduced the levels of ROS which led to reduced oxidative stress as evidenced by decreased production of MDA, which otherwise was higher due to lipid peroxidation in MG treated NRK-52E cells. Chronic hyperglycaemia, if unmanaged not only culminates into various complications but also leads to pancreatic β-cell death. In a recent study, it was shown that MG leads to β-cell death by the formation of AGEs [57]. We hence, looked for the NRK-52E cell death caused due to MG and if SM could prevent the same. Interestingly, SM could prevent the cell death caused due to MG as seen by reduced %DNA in the

tail. The apoptosis in NRK-52E could be either due to the formation of AGEs or the oxidative stress due to MG.

The MG mediated AGEs could readily interact with their membrane-bound receptor RAGE and result in kidney dysfunction by inducing chronic inflammation. In a study on OVE26 mouse, it was shown that RAGE deletion could prevent renal function in diabetic mice, thereby explaining the role RAGE plays in DN [58]. Therefore elucidating the role of SM in MG-mediated RAGE expression became crucial, and we found that SM could decrease the mRNA expression of RAGE as compared to that of MG-treated cells. The activation of RAGE due to AGEs can lead to various inflammatory reactions as discussed earlier, by inducing the expressions of inflammatory markers like NADPH oxidase, TNF-α, IL-1β, IL-6, which gets accelerated due to the expression of cellular adhesion molecules like ICAM-1 [59]. In the current study, we found that treatment of MG not only induced the up regulated expression of pro-inflammatory cytokines like TNF-α, IL-1β, IL-6, but also of NADPH oxidase and ICAM-1, which was ameliorated in the cells treated with SM along with MG. The interaction of RAGE with AGEs can lead to the generation of ROS via NADPH oxidase which can promote the expression of TGF-β via NFκB, mitogen-activated protein kinase (MAPK), or PKC pathways in mesangial and renal tubulointerstitial cells in the kidneys [60]. TGF- β being a pro-fibrotic cytokine plays a very crucial role in renal fibrosis via EMT. We found that MG exposure changed the epithelial morphology of NRK-52E to more extended, fibroblast-like morphology, possibly due to higher mRNA expression of TGF- β as compared to lower expression of TGF- β in the cells co-treated with SM and MG. Our results are in agreement with a previous study, where TGF- β led to fibrosis of renal proximal tubules cells, leading to the death of the cells [61].

Conclusion

SM was isolated in the lab and upon characterization by various methods, its similarity with the standard SM was confirmed. Further, the present study identifies SM to be an inhibitor for AGEs and hence could be used to understand its role in the prevention of diabetes and its complications like nephropathy, neuropathy, etc. Also, as compared to metformin, it has proven to be a better inhibitor for AGEs. Here, our *in vitro* studies with NRK-52E cells demonstrate that SM was able to prevent the DN by significantly reducing the ROS production in the cells. SM could also reduce the formation of pro-inflammatory cytokines and also cell death of NRK-52E cells. The results of MG exposure and treatment with SM at protein levels needs further investigation. Also, future *in vivo* experiments for exploring the preventing role of SM in DN can provide a better understanding of the role of SM in preventing DN at the systemic level.

Abbreviations

AGE**,** Advanced glycation end product; TLC, Thin-layer chromatography; HPLC, High-performance liquid chromatography; FTIR, Fourier-transform infrared spectroscopy; LC-MS, Liquid chromatography – Mass spectra; PDA, Photodiode detector; v/v, volume/volume; SEM, Standard Error of Mean; BSA, Bovine Serum Albumin; SOD, Superoxide dismutase; ROS, Reactive oxidative species; KBr, Potassium bromide; MG, Methylglyoxal; RAGE, Receptor for advanced glycation end product

Declarations

Acknowledgments

The author would like to acknowledge Charotar University of Science and Technology for providing the author with CHARUSAT Ph.D. Scholar Fellowship (CPSF).

Author contributions

The design and conception of the study was done by K.P. F.P. and P.M. K.P. did the acquisition of the data. Analysis and/or interpretation of data was done by K.P., .F.P and P.M. The drafting of the manuscript was done by K.P. and F.P. while revising the manuscript critically for important intellectual content was done by K.P., F. P., D.P., and P.M. All authors have read and approved the manuscript.

Competing interests

The authors declare no competing interests.

Data availability

All data generated or analysed during the current study are included in the manuscript.

References

1. Writing team for the Diabetes Control and Complications Trial/Epidemiology of Diabetes Interventions and Complications Research Group. Sustained effect of intensive treatment of type 1 diabetes mellitus on development and progression of diabetic nephropathy: the Epidemiology of Diabetes Interventions and Complications (EDIC) study. *JAMA*290, 2159-2167 (2003).
2. Fioretto, P., Steffes, M.W., Sutherland, D.E., Goetz, F.C. and Mauer, M. Reversal of lesions of diabetic nephropathy after pancreas transplantation. *Engl. J. Med.* **339**, 69-75 (1998).
3. Barbosa, J., Steffes, M.W., Sutherland, D.E., Connett, J.E., Rao, K.V. and Mauer, S.M.. Effect of glycemic control on early diabetic renal lesions: A 5-year randomized controlled clinical trial of insulin-dependent diabetic kidney transplant recipients. *JAMA* **272**, 600-606 (1994).
4. Yao, D. and Brownlee, M. Hyperglycemia-induced reactive oxygen species increase expression of the receptor for advanced glycation end products (RAGE) and RAGE ligands. *Diabetes***59,** 249-255 (2010).

5. Neglia, C.I., Cohen, H.J., Garber, A.R., Ellis, P.D., Thorpe, S.R. and Baynes, J.W. 13C NMR investigation of nonenzymatic glucosylation of protein. Model studies using RNase A. *Biol. Chem*. **258** 14279-14283 (1983).

6. Lapolla, A., Traldi, P. and Fedele, D. Importance of measuring products of non-enzymatic glycation of proteins. *Biochem.***38,** 103-115 (2005).

7. Kilhovd, B.K., et al.,. Increased serum levels of the specific AGE-compound methylglyoxal-derived hydroimidazolone in patients with type 2 diabetes. *Metabolism***52**, 163-167 (2003).

8. Cooper, M.E. Interaction of metabolic and haemodynamic factors in mediating experimental diabetic nephropathy. *Diabetologia*, 44, 1957-1972 (2001).

9. Pasupulati, A.K., Chitra, P.S. and Reddy, G.B. Advanced glycation end products mediated cellular and molecular events in the pathology of diabetic nephropathy. *concepts*, **7**, 293-309 (2016).

10. Ceriello A, et al., Total radical-trapping antioxidant parameter in NIDDM patients. *Diabetes Care***20**, 194–197 (1997).

11. Kang, J.H. Modification and inactivation of human Cu, Zn-superoxide dismutase by methylglyoxal. *Cells***15,** 194-199 (2003).

12. Najjar, F.M., Taghavi, F., Ghadari, R., Sheibani, N. and Moosavi-Movahedi, A.A.,. Destructive effect of non-enzymatic glycation on catalase and remediation via curcumin. *Biochem. Biophys.***630**,81-90 (2017).

13. Choudhary, M.I., Maher, S., Begum, A., Abbaskhan, A., Ali, S. and Khan, A. Characterization and antiglycation activity of phenolic constituents from Viscum album (European Mistletoe). *Pharma. Bull (Tokyo)*, **58**, 980-982 (2010).

14. Meng, G., Zhu, H., Yang, S., Wu, F., Zheng, H., Chen, E. and Xu, J. Attenuating effects of Ganoderma lucidum polysaccharides on myocardial collagen cross-linking relates to advanced glycation end product and antioxidant enzymes in high-fat-diet and streptozotocin-induced diabetic rats. *Polym.* **84**, 180-185 (2011).

15. Sun, Z., Peng, X., Liu, J., Fan, K.W., Wang, M. and Chen, F. Inhibitory effects of microalgal extracts on the formation of advanced glycation endproducts (AGEs). *Food chemistry*, **120**, 261-267 (2010).

16. Yazdanparast, R., Ardestani, A. and Jamshidi, S. Experimental diabetes treated with Achillea santolina: effect on pancreatic oxidative parameters. *Ethnopharmacol.***112**, 13-18 (2007).

17. Murali, B., Upadhyaya, U.M. and Goyal, R.K. Effect of chronic treatment with Enicostemma littorale in non-insulin-dependent diabetic (NIDDM) rats. *Ethnopharmacol.***81**, 199-204 (2002).

18. Yamahara, J., Kobayashi, M., Matsuda, H. and Aoki, S. Anticholinergic action of Swertia japonica and an active constituent. *Ethnopharmacol.***33**, 31-35 (1991)

19. Vaidya, H., Rajani, M., Sudarsanam, V., Padh, H. and Goyal, R. Antihyperlipidaemic activity of swertiamarin, a secoiridoid glycoside in poloxamer-407-induced hyperlipidaemic rats. *Nat. Med.* 63(4), 437-442 (2009).

20. Vaidya, H., Prajapati, A., Rajani, M., Sudarsanam, V., Padh, H. and Goyal, R.K. Beneficial Effects of Swertiamarin on Dyslipidaemia in Streptozotocin-induced Type 2 Diabetic Rats. *Res.* **26**, 1259-1261 (2012).

21. Jaishree, V. and Badami, S. Antioxidant and hepatoprotective effect of swertiamarin from Enicostemma axillare against D-galactosamine induced acute liver damage in rats. *Ethnopharmacol.***130**, 103-106 (2010).

22. Nakagawa, T., Yokozawa, T., Terasawa, K., Shu, S. and Juneja, L.R. Protective activity of green tea against free radical-and glucose-mediated protein damage. *Agric. Food Chem.***50**, 2418-2422 (2002).

23. Kshirsagar, P.R., Pai, S.R., Nimbalkar, M.S. and Gaikwad, N.B. RP-HPLC analysis of seco-iridoid glycoside swertiamarin from different Swertia species. *Prod. Res.* **30**, 865-868 (2016).

24. McPherson, J.D., Shilton, B.H. and Walton, D.J. Role of fructose in glycation and cross-linking of proteins. *Biochemistry***27**, 1901-1907 (1988).

25. Allarakha, S., Ahmad, P., Ishtikhar, M., Zaheer, M.S., Siddiqi, S.S. and Ali, A. Fructosylation generates neo-epitopes on human serum albumin. *IUBMB life*, **67**, 338-347 (2015).

26. Riss, T. L., et al. Cell viability assays. In: G.S. Sittampalam, N.P. Coussens, H. Nelson, et al., eds. Assay guidance manual Bethesda (MD): Eli Lilly & Company and the National Center for Advancing Translational Sciences. (2013). Available from: http://www.ncbi.nlm.nih.gov/books/NBK144065/

27. Wilker, S.C., Chellan, P., Arnold, B.M. and Nagaraj, R.H. Chromatographic quantification of argpyrimidine, a methylglyoxal-derived product in tissue proteins: comparison with pentosidine. *Biochem.***290**, 353-358 (2001).

28. Karbowski, M., Kurono, C., Wozniak, M., Ostrowski, M., Teranishi, M., Nishizawa, Y., Usukura, J., Soji, T. and Wakabayashi, T. Free radical–induced megamitochondria formation and apoptosis. *Free Radic. Biol. Med.* **26**, 396-409 (1999).

29. Tukozkan, N., Erdamar, H. and Seven, I. Measurement of total malondialdehyde in plasma and tissues by high-performance liquid chromatography and thiobarbituric acid assay. *Firat Tip Dergisi*, **11**, 88-92 (2006).

30. Fazeli, G., Stopper, H., Schinzel, R., Ni, C.W., Jo, H. and Schupp, N. Angiotensin II induces DNA damage via AT1 receptor and NADPH oxidase isoform Nox4. *Mutagenesis***27**, 673-681 (2012).

31. Rana, V.S., Dhanani, T. and Kumar, S. Improved and Rapid HPLC-PDA Method for Identification and Quantification of Swertiamarin in the Aerial Parts of Enicostemma Axillare. *Malaysian Journal of Pharmaceutical Sciences***10**, 1-10 (2012).

32. Vishwakarma, S., Rajani, M., Bagul, M. and Goyal, R. A rapid method for the isolation of swertiamarin from Enicostemma littorale. *Biol.***42**, 400-403 (2004).

33. Kumar, S. and Jairaj, V. An effective method for isolation of pure swertiamarin from Enicostemma littorale blume. *Indo Global J Pharmaceutical Sci*, **8**, 1-8 (2018).

34. Wu, T., Li, J., Li, Y. and Song, H. Antioxidant and hepatoprotective effect of swertiamarin on carbon tetrachloride-induced hepatotoxicity via the Nrf2/HO-1 pathway. *Physiol. Biochem.**41***, 2242-2254 (2017).

35. Nita, M. and Grzybowski, A. The role of the reactive oxygen species and oxidative stress in the pathomechanism of the age-related ocular diseases and other pathologies of the anterior and posterior eye segments in adults. *Med. Cell. Longev.* (2016).

36. Fukami, K., Yamagishi, S.I., Ueda, S. and Okuda, S. Role of AGEs in diabetic nephropathy. *Pharm. Des.***14**, 946-952 (2008).

37. Ahmed, N. Advanced glycation endproducts—role in pathology of diabetic complications. *Diabetes Res. Clin. Pract.***67**, 3-21 (2005).

38. Singh, V.P., Bali, A., Singh, N. and Jaggi, A.S. Advanced glycation end products and diabetic complications. *Korean J. Physiol. Pharmacol.***18,** 1-14 (2014).

39. Lunceford, N. & Gugliucci, A. Ilex paraguariensis extracts inhibit AGE formation more efficiently than green tea. *Fitoterapia***76**, 419–427 (2005).

40. Lapolla, A., et al. Glyoxal and methylglyoxal levels in diabetic patients: quantitative determination by a new GC/MS method. *Chem. Lab. Med.***41,** 1166-1173 (2003).

41. Stinghen, A.E., Massy, Z.A., Vlassara, H., Striker, G.E. and Boullier, A. Uremic toxicity of advanced glycation end products in CKD. *Am. Soc. Nephrol.***27**, 354-370 (2016).

42. Henning, C., Liehr, K., Girndt, M., Ulrich, C. and Glomb, M.A. Extending the spectrum of α-dicarbonyl compounds in vivo. *Biol. Chem.***289**, 28676-28688 (2014.).

43. Wang, W., Yagiz, Y., Buran, T.J., do Nascimento Nunes, C. and Gu, L. Phytochemicals from berries and grapes inhibited the formation of advanced glycation end-products by scavenging reactive

carbonyls. *Food research international***44**, 2666-2673 (2011).

44. Justino, A.B., Franco, R.R., Silva, H.C., Saraiva, A.L., Sousa, R.M. and Espindola, F.S. B procyanidins of Annona crassiflora fruit peel inhibited glycation, lipid peroxidation and protein-bound carbonyls, with protective effects on glycated catalase. *Rep.***9**, 1-15 (2019.).

45. Ardestani, A. and Yazdanparast, R. Cyperus rotundus suppresses AGE formation and protein oxidation in a model of fructose-mediated protein glycoxidation. *J. Biol. Macromol.***41**, 572-578 (2007).

46. Ahmad, S., Shahab, U., Baig, M.H., Khan, M.S., Khan, M.S., Srivastava, A.K. and Saeed, M. Inhibitory effect of metformin and pyridoxamine in the formation of early, intermediate and advanced glycation end-products. *PloS ONE*, **8**, p.e72128 (2013).

47. Ishibashi, Y., Matsui, T., Takeuchi, M. and Yamagishi, S. Metformin inhibits advanced glycation end products (AGEs)-induced renal tubular cell injury by suppressing reactive oxygen species generation via reducing receptor for AGEs (RAGE) expression. *Metab. Res.***44**, 891-895 (2012).

48. Jairajpuri, D. S., Fatima, S., and Saleemuddin, M. Immunoglobulin glycation with fructose: a comparative study. *Chim. Acta.***378**, 86–92 (2007).

49. Allarakha, S., Ahmad, P., Ishtikhar, M., Zaheer, M.S., Siddiqi, S.S. and Ali, A. Fructosylation generates neo-epitopes on human serum albumin. *IUBMB life*, 67, 338-347 (2015).

50. Yan, H. & Harding, J. J. Glycation-induced inactivation and loss of antigenicity of catalase and superoxide dismutase. *J.***328**(Pt 2), 599–605 (1997).

51. Ha, H., Hwang, I.A., Park, J.H. and Lee, H.B. Role of reactive oxygen species in the pathogenesis of diabetic nephropathy. *Diabetes Res. Clin. Pract.***82**, S42-S45 (2008).

52. Liu, Bing-Fen et al. Methylglyoxal induces apoptosis through activation of p38 mitogen-activated protein kinase in rat mesangial cells. Kidney Int. **63**, 947 – 957 (2003).

53. Oya, T., Hattori, N., Mizuno, Y., Miyata, S., Maeda, S., Osawa, T. and Uchida, K. Methylglyoxal modification of protein chemical and immunochemical characterization of methylglyoxal-arginine adducts. *Biol. Chem.***274**, 18492-18502 (1999).

54. Padival, A.K., Crabb, J.W. and Nagaraj, R.H. Methylglyoxal modifies heat shock protein 27 in glomerular mesangial cells. *FEBS Lett.***551**, 113-118 (2003).

55. Niki, E. Lipid peroxidation products as oxidative stress biomarkers. *Biofactors***34**, 171–180 (2008).

56. Ayala, A., Muñoz, M.F. and Argüelles, S.,. Lipid peroxidation: production, metabolism, and signaling mechanisms of malondialdehyde and 4-hydroxy-2-nonenal. Oxid. Med. Cell. Longev. (2014).

57. Sompong, W., Cheng, H. and Adisakwattana, S. Ferulic acid prevents methylglyoxal-induced protein glycation, DNA damage, and apoptosis in pancreatic β-cells. *Physiol. Biochem.***73**, 121-131 (2017).

58. Reiniger, N., et al. Deletion of the receptor for advanced glycation end products reduces glomerulosclerosis and preserves renal function in the diabetic OVE26 mouse. *Diabetes*, **59**, 2043-2054 (2010).

59. Ye, S.D., et al. Intensive insulin therapy decreases urinary MCP-1 and ICAM-1 excretions in incipient diabetic nephropathy. *J. Clin. Invest.***39**, 980-985 (2009).

60. Yamagishi, S.I., Inagaki, Y., Okamoto, T., Amano, S., Koga, K., Takeuchi, M. and Makita, Z. Advanced glycation end product-induced apoptosis and overexpression of vascular endothelial growth factor and monocyte chemoattractant protein-1 in human-cultured mesangial cells*. J. Biol. Chem.***277**, 20309-20315 (2002).

61. Hung, T.J., et al. 20-Hydroxyecdysone attenuates TGF-β1-induced renal cellular fibrosis in proximal tubule cells. *Diabetes Complications*, **26**, 463-469 (2012).

Figures

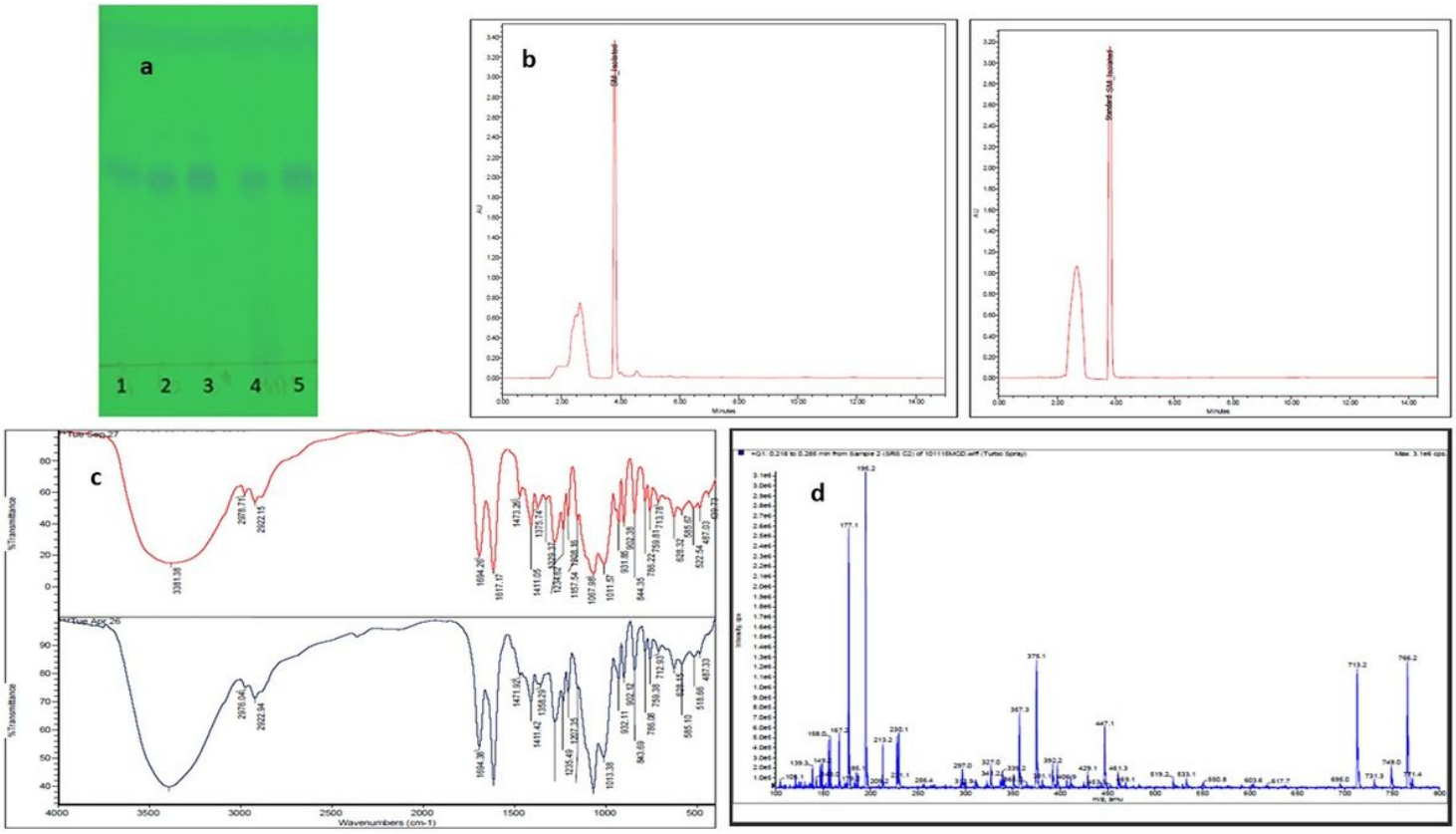

Figure 1

(a) TLC profile: Lane 1, 2: Fractions containing SM along with impurities. Lane3: Standard Lane 4: Methanolic extract of E.littorale Lane 5: Fraction containing SM in the TLC mobile phase (Chloroform: methanol in 8:2 v/v proportion) (b) The HPLC chromatogram of SM isolated in the lab (a) and of the standard SM (b) at 1 mg/ml using acetonitrile: water (10:90) as the mobile phase. (c) An overlay of FT-IR spectrum of standard SM (red) and SM isolated in the lab (blue). (d) The mass spectrum of isolated swertiamarin showing characteristic m/z of 375.1.

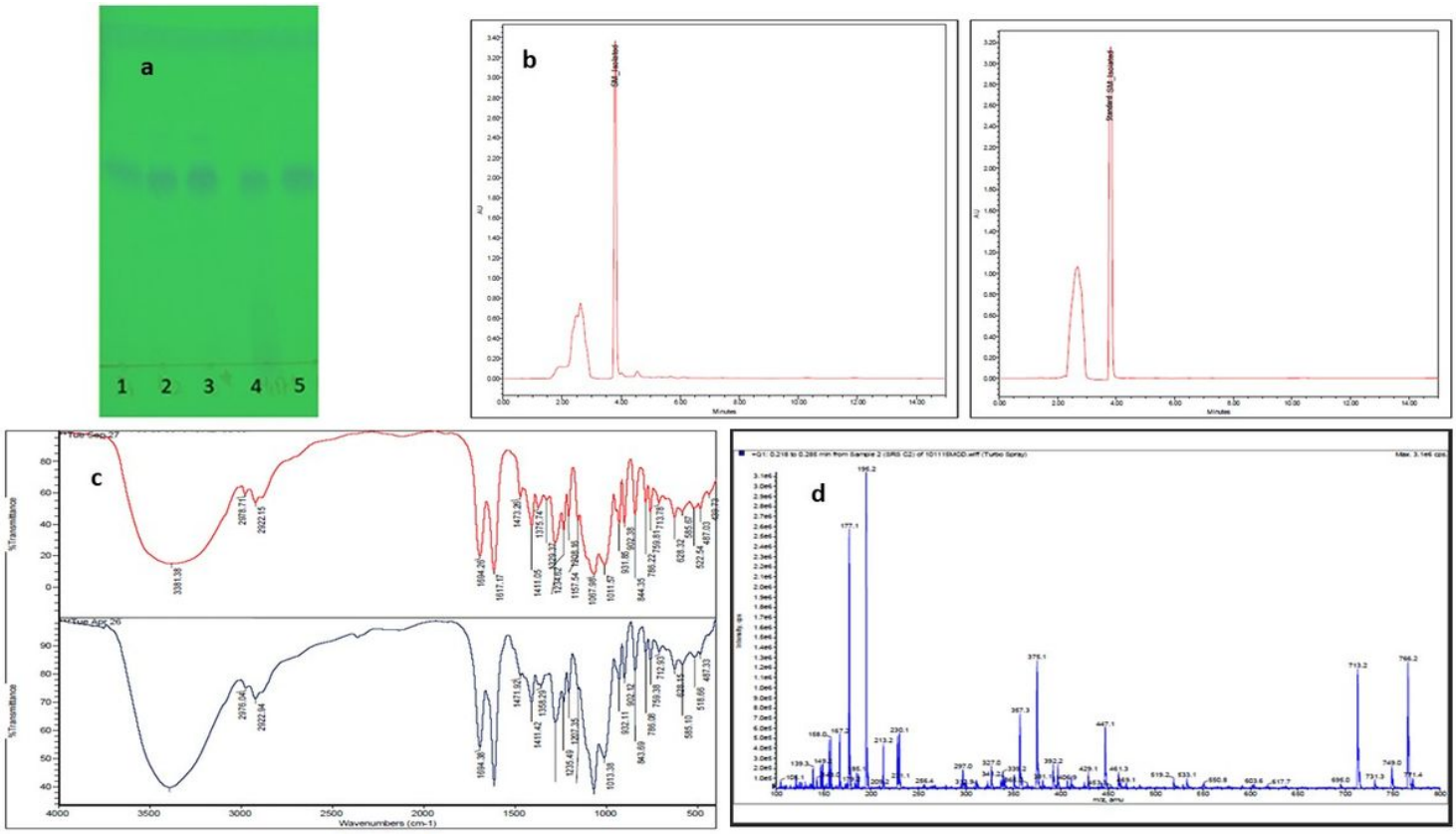

Figure 1

(a) TLC profile: Lane 1, 2: Fractions containing SM along with impurities. Lane3: Standard Lane 4: Methanolic extract of E.littorale Lane 5: Fraction containing SM in the TLC mobile phase (Chloroform: methanol in 8:2 v/v proportion) (b) The HPLC chromatogram of SM isolated in the lab (a) and of the standard SM (b) at 1 mg/ml using acetonitrile: water (10:90) as the mobile phase. (c) An overlay of FT-IR spectrum of standard SM (red) and SM isolated in the lab (blue). (d) The mass spectrum of isolated swertiamarin showing characteristic m/z of 375.1.

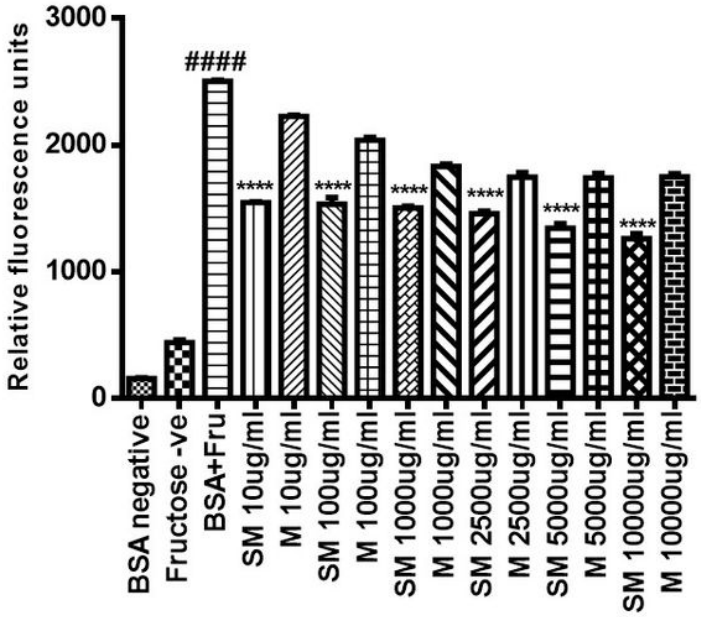

Figure 2

The intensity of fluorescence of AGEs in the presence and absence of swertiamarin (SM) and its comparison with metformin (M) at different concentrations measured using an excitation wavelength of 370 nm and an emission wavelength of 440 nm. The results are Mean ± SEM of 3 individual experiments. ****p<0.0001

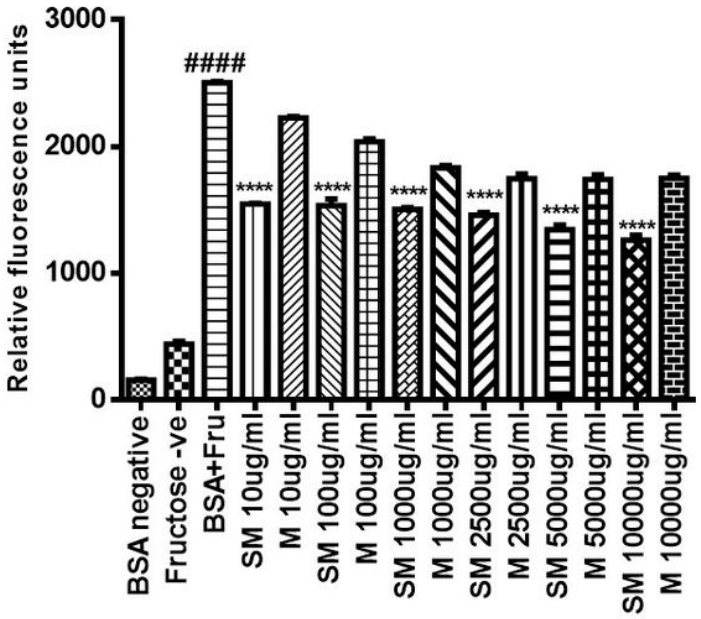

Figure 2

The intensity of fluorescence of AGEs in the presence and absence of swertiamarin (SM) and its comparison with metformin (M) at different concentrations measured using an excitation wavelength of 370 nm and an emission wavelength of 440 nm. The results are Mean ± SEM of 3 individual experiments. ****p<0.0001

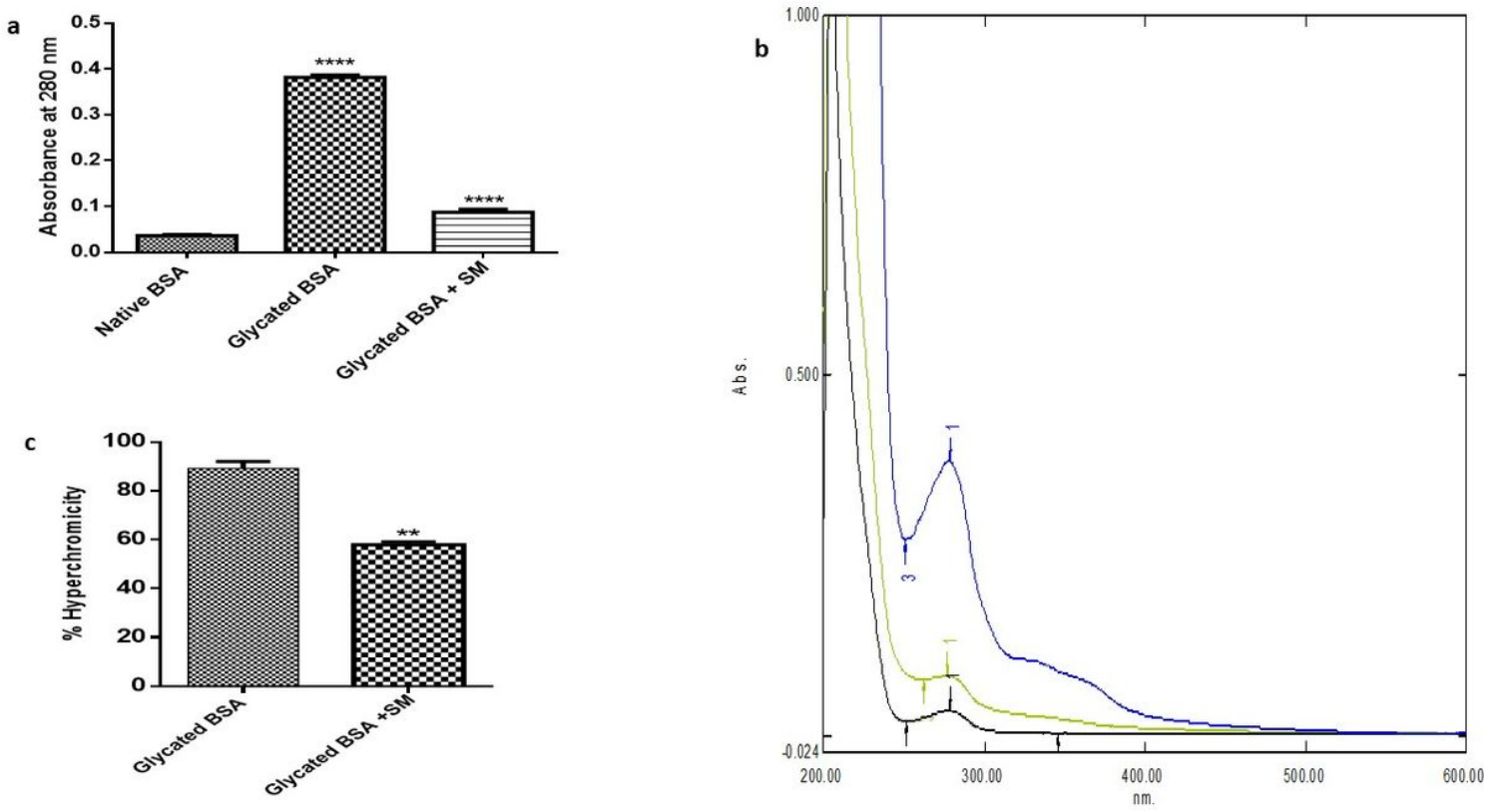

Figure 3

Antiglycative effect of swertiamarin at 100 µg/ml (SM 100) as shown by absorbance at 280nm using UV-spectrophotometer (a), the structural changes as seen by the shift in the peaks due to glycation (b), suggesting hyperchromicity (c). The results are Mean ± SEM of 3 individual experiments. ****p<0.0001, **p<0.054.

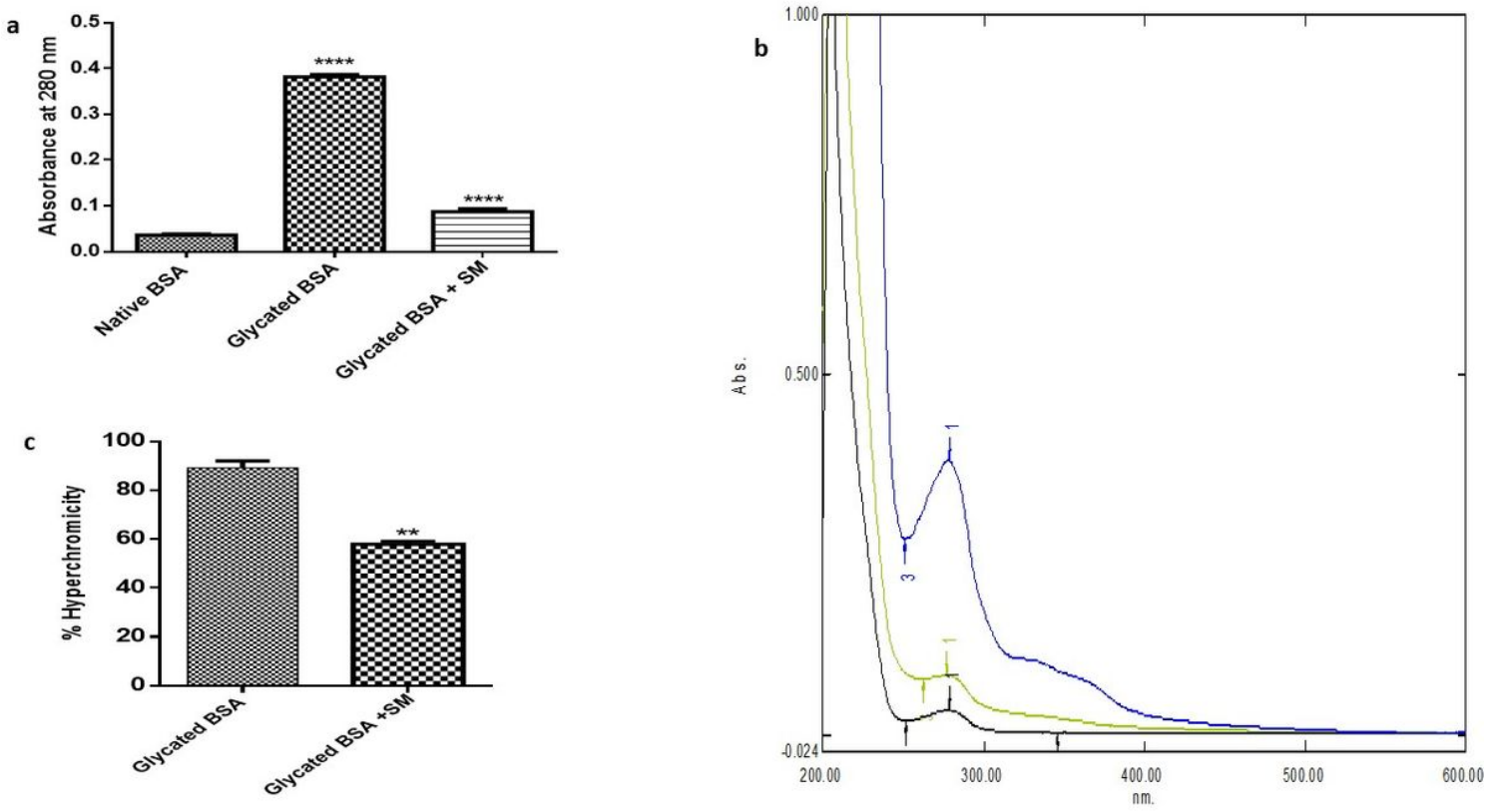

Figure 3

Antiglycative effect of swertiamarin at 100 µg/ml (SM 100) as shown by absorbance at 280nm using UV-spectrophotometer (a), the structural changes as seen by the shift in the peaks due to glycation (b), suggesting hyperchromicity (c). The results are Mean ± SEM of 3 individual experiments. ****p<0.0001, **p<0.054.

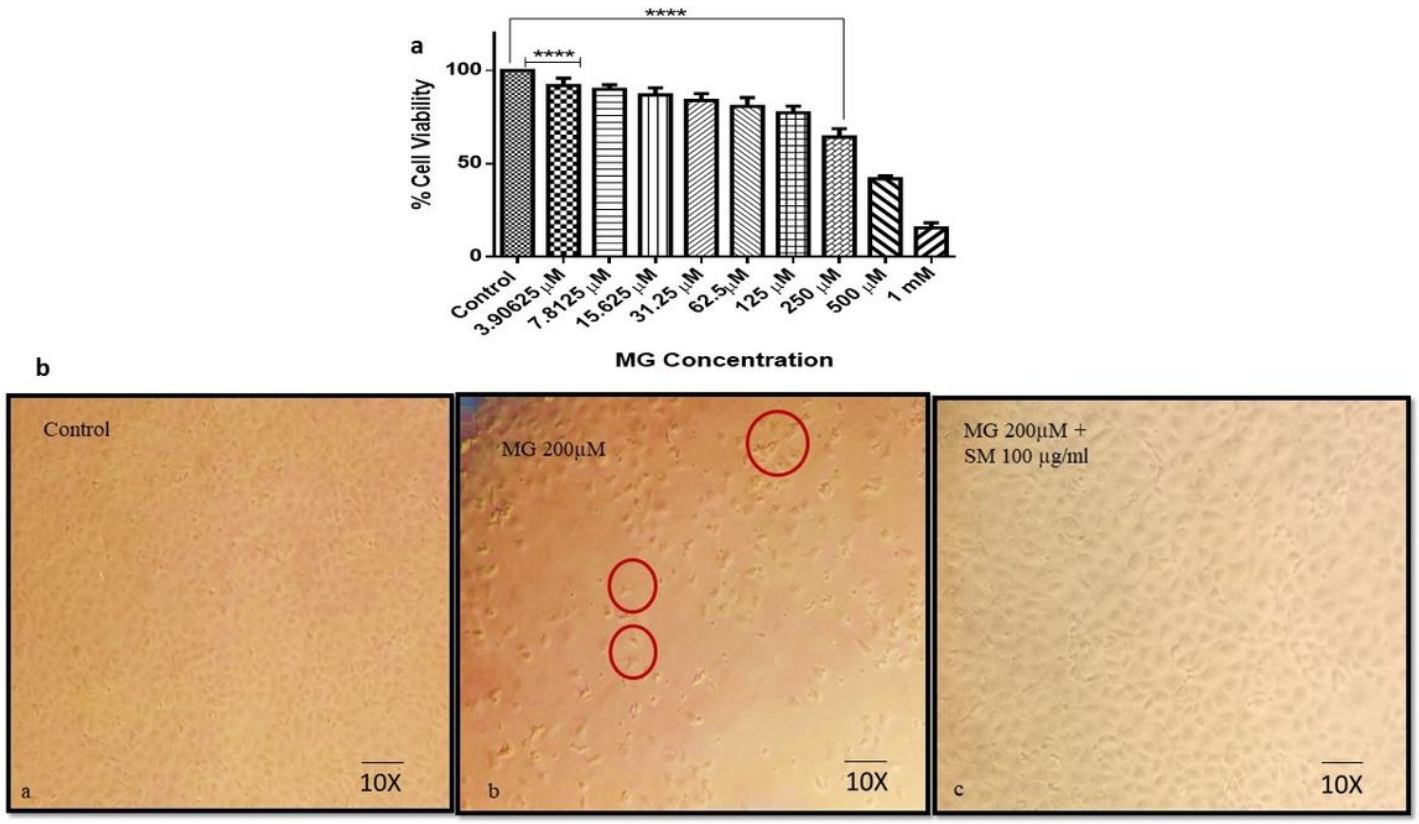

Figure 4

(a)The effect MG on the cell viability in NRK-52E cells. NRK-52E cells when treated with different concentrations of MG caused cell death in a dose-dependent manner as compared to control ****p<0.0001. (b) Morphology of NRK-52E cells in each treatment group at 24 h. SM improved MG induced morphological changes in NRK-52E cells. Control NRK-52E cells show epithelial morphology while MG treatment changes the morphology to a fibroblast-like appearance which is prevented by SM.

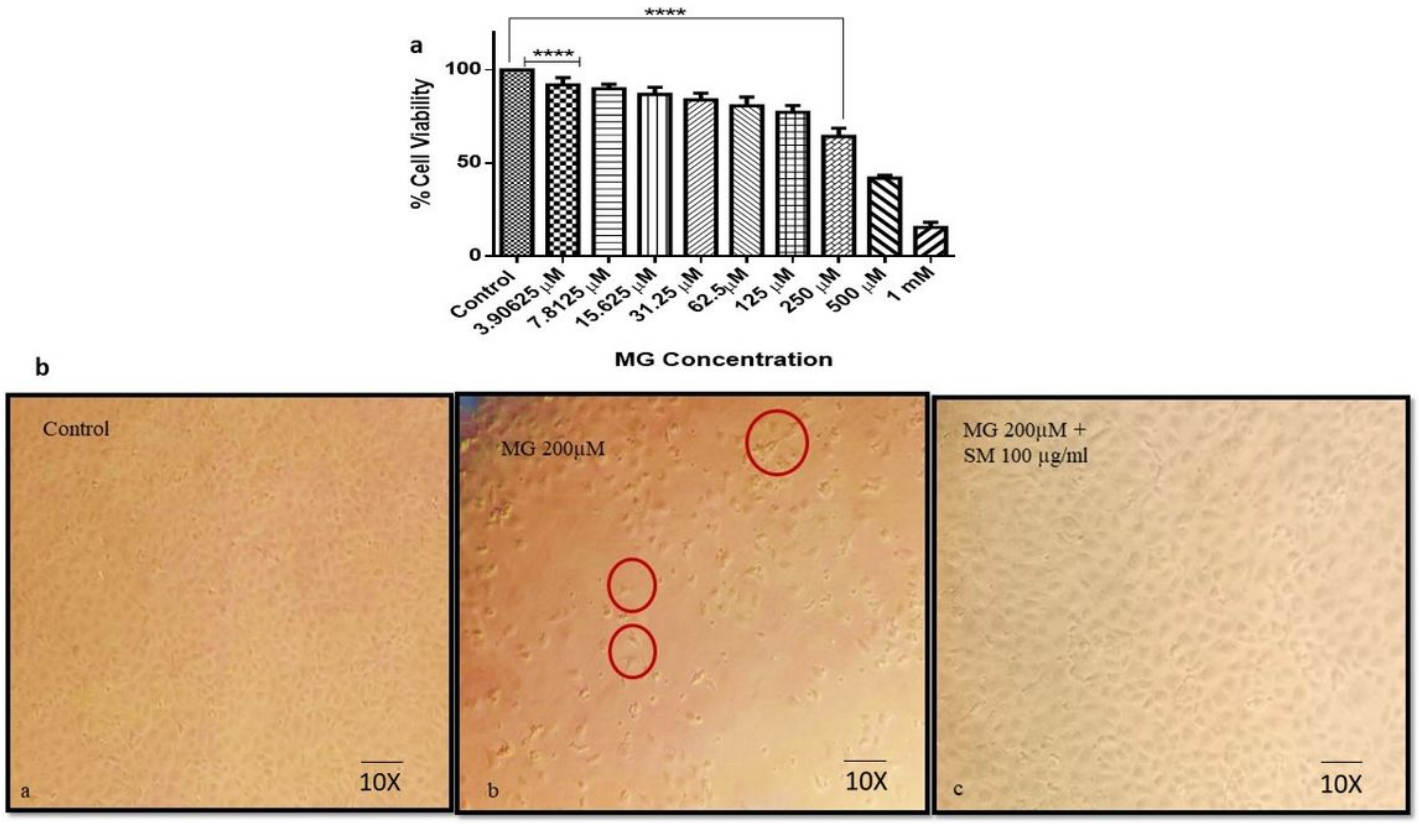

Figure 4

(a)The effect MG on the cell viability in NRK-52E cells. NRK-52E cells when treated with different concentrations of MG caused cell death in a dose-dependent manner as compared to control ****p<0.0001. (b) Morphology of NRK-52E cells in each treatment group at 24 h. SM improved MG induced morphological changes in NRK-52E cells. Control NRK-52E cells show epithelial morphology while MG treatment changes the morphology to a fibroblast-like appearance which is prevented by SM.

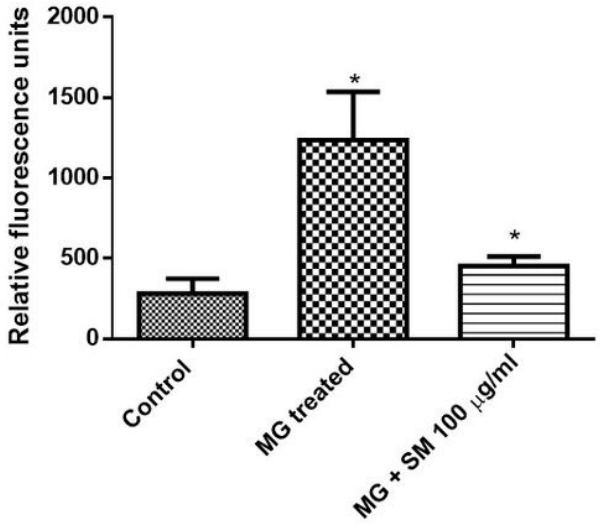

Figure 5

Detection of argpyrimidine levels. As compared to control, treatment of MG in the NRK-52E cells led to the formation of argpyrimindine by MG-induced modifications of arginine which could be prevented in MG and SM co-treatment group (*p <0.05).

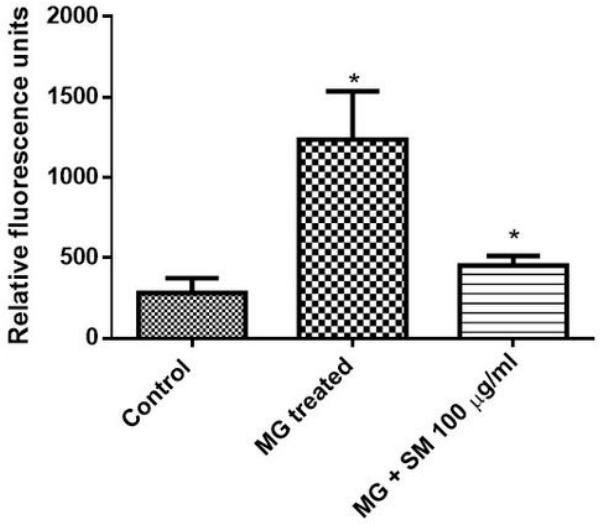

Figure 5

Detection of argpyrimidine levels. As compared to control, treatment of MG in the NRK-52E cells led to the formation of argpyrimindine by MG-induced modifications of arginine which could be prevented in MG and SM co-treatment group (*p <0.05).

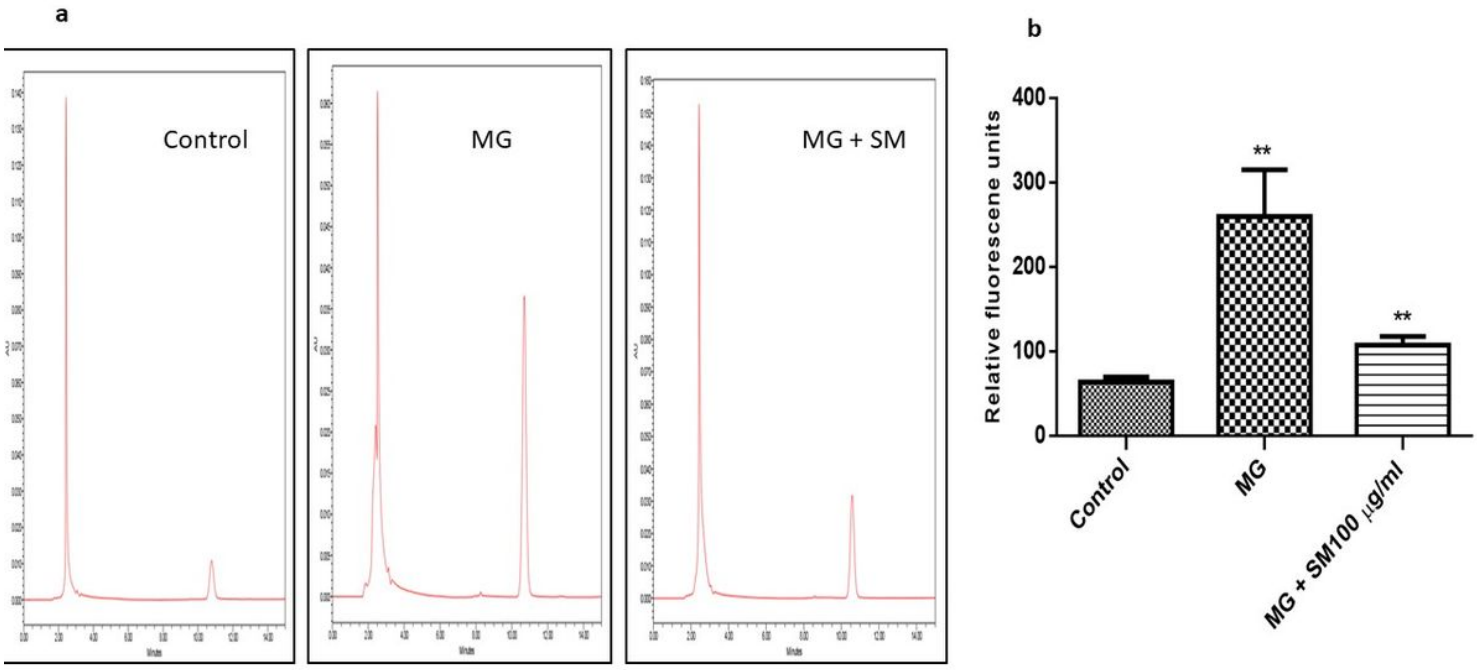

Figure 6

(a) HPLC chromatograms of total MDA measured in various groups. The MDA estimation was done using DNPH derivatization of the cell lysate, loaded on ODS2 C18 reverse phase column using Acetonitrile-distilled water (38:62) containing 0.2% acetic acid as the mobile phase. As compared to control cells, MDA levels are higher in MG treated sample and co-treatment with MG and SM group reduced the levels of MDA. (b) Effect of MG and SM on ROS generation. MG induced the formation of ROS in NRK-52E cells, which upon co-treatment of SM with MG was significantly reduced. (**$p<0.01$).

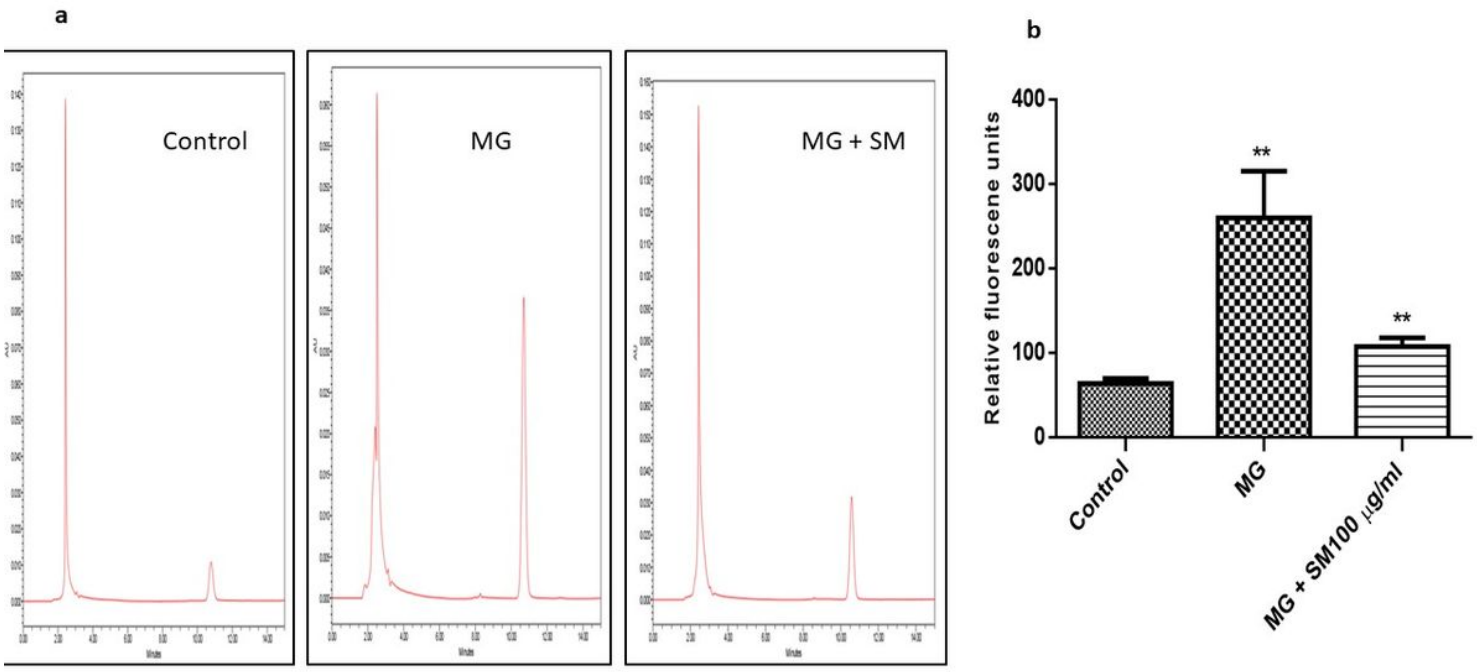

Figure 6

(a) HPLC chromatograms of total MDA measured in various groups. The MDA estimation was done using DNPH derivatization of the cell lysate, loaded on ODS2 C18 reverse phase column using Acetonitrile-distilled water (38:62) containing 0.2% acetic acid as the mobile phase. As compared to control cells, MDA levels are higher in MG treated sample and co-treatment with MG and SM group reduced the levels of MDA. (b) Effect of MG and SM on ROS generation. MG induced the formation of ROS in NRK-52E cells, which upon co-treatment of SM with MG was significantly reduced. (**$p<0.01$).

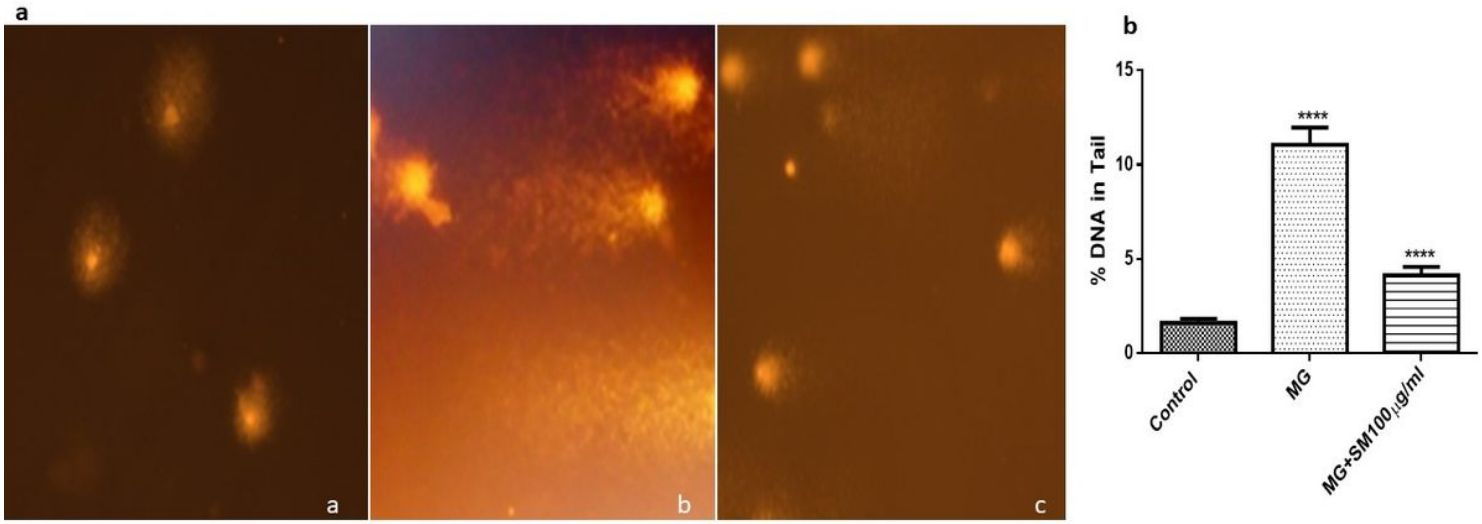

Figure 7

(a) Representative image of comet formed in different groups showing DNA damage by tailing. (b) shows the graph of % DNA in the tail in different groups. The % DNA in the tail is significantly higher in MG exposed group as compared to SM and MG group (****p <0.0001).

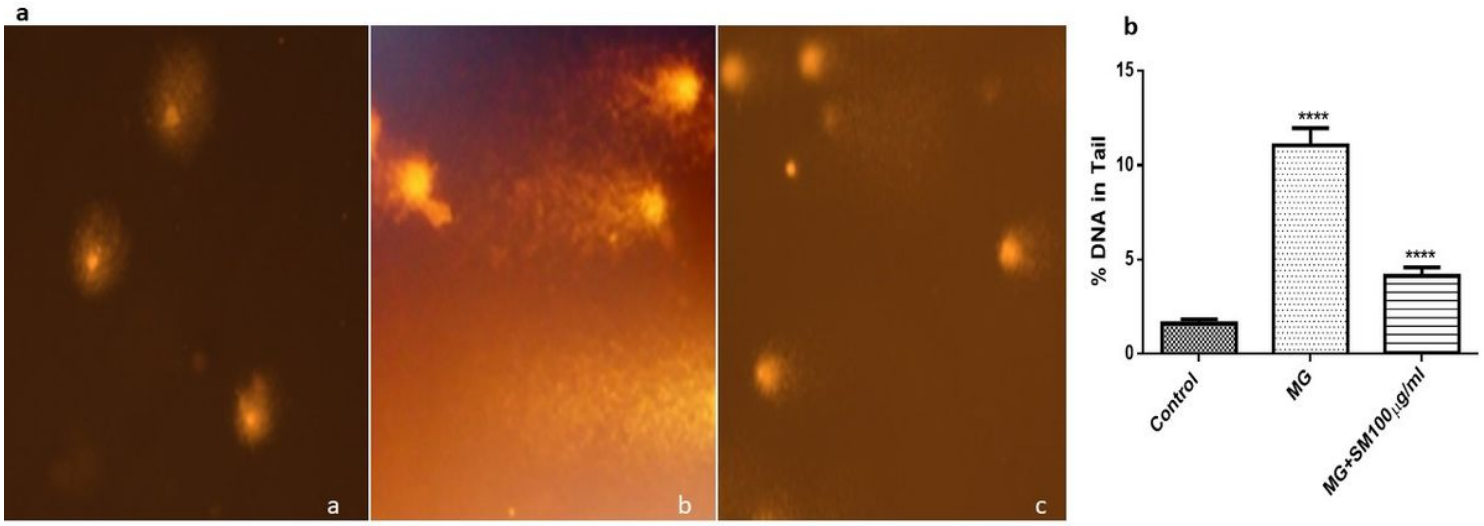

Figure 7

(a) Representative image of comet formed in different groups showing DNA damage by tailing. (b) shows the graph of % DNA in the tail in different groups. The % DNA in the tail is significantly higher in MG exposed group as compared to SM and MG group (****p <0.0001).

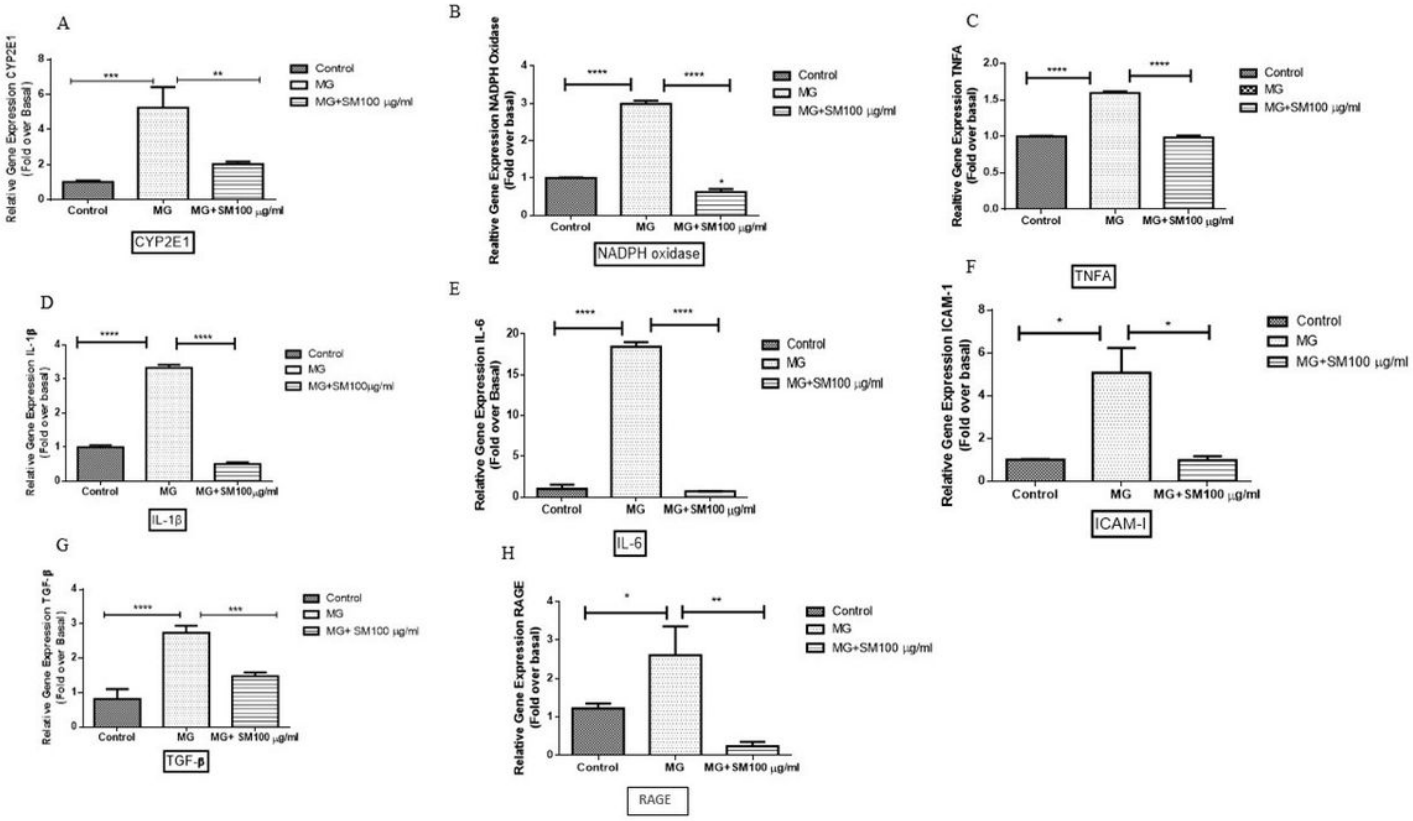

Figure 8

qRT-PCR analysis results of (A) CYP2E1 (B) NADPO (C) TNF-α (D) IL-1β (E) IL-6, (F) ICAM-1 (G) TGF- β and (H) RAGE genes from MG-exposed and SM treated NRK-52E cells The level of gene expression was calculated after normalizing against 18 S in each sample and is presented as relative mRNA expression units. Results are means ± SEM (3 individual experiments). p values compared to control untreated cells. *p<0.05, **p<0.01 ***p<0.001, and ****p<0.0001.

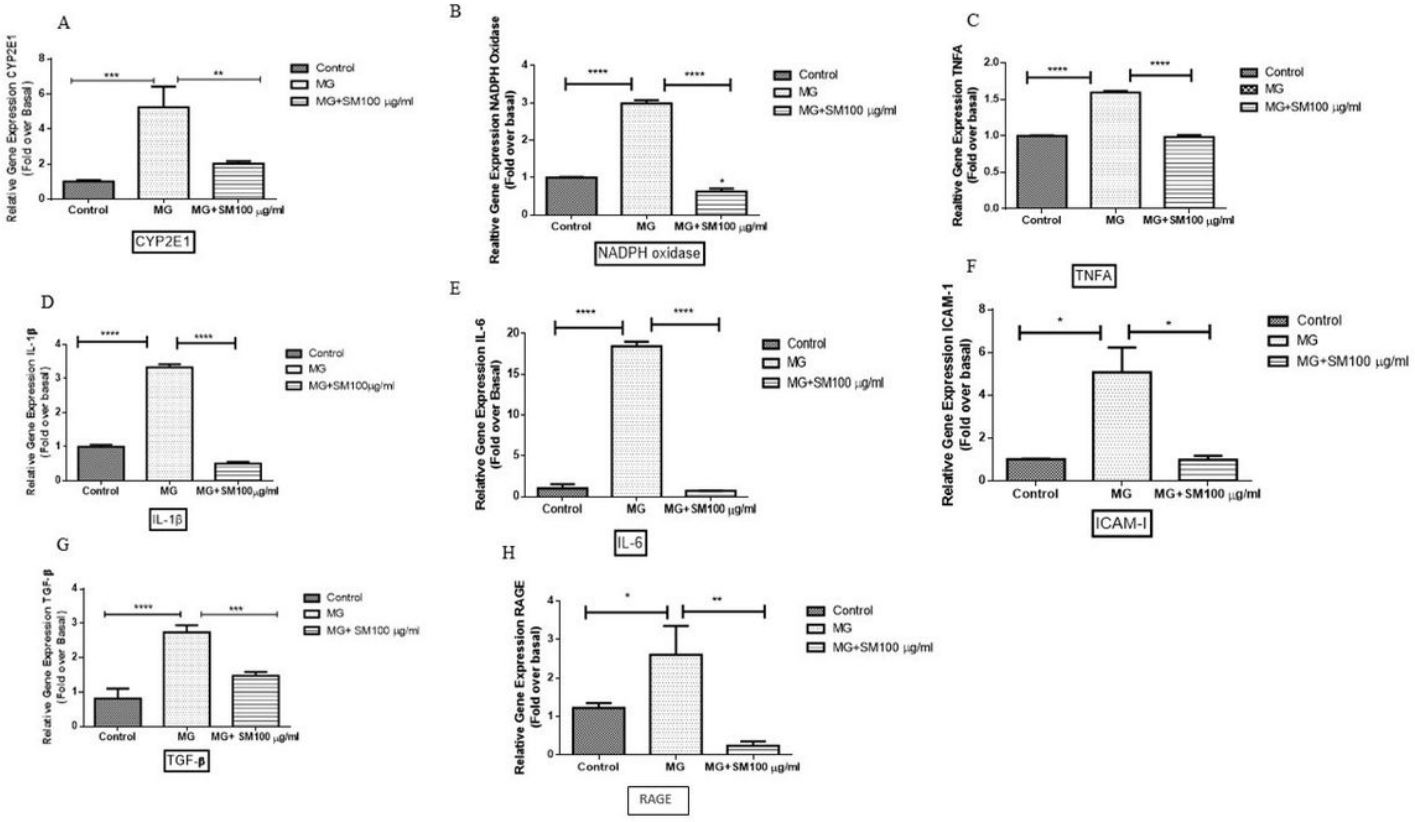

Figure 8

qRT-PCR analysis results of (A) CYP2E1 (B) NADPO (C) TNF-α (D) IL-1β (E) IL-6, (F) ICAM-1 (G) TGF- β and (H) RAGE genes from MG-exposed and SM treated NRK-52E cells The level of gene expression was calculated after normalizing against 18 S in each sample and is presented as relative mRNA expression units. Results are means ± SEM (3 individual experiments). p values compared to control untreated cells. *p<0.05, **p<0.01 ***p<0.001, and ****p<0.0001.